Efficient hydrogen peroxide reduction in glutathione peroxidase cycle using cost-effective FeSe$_2$ nanospheres

Saif Khan[1]*, Sundeep S. Bhagwath[1], Mohammad Rehan Ajmal[2], Intikhab A. Ansari[3], Mohtashim Lohani[4], Sanjaya Pavgada Raghunandana[1] and Mohammad Luqman[5]*

[1]Department of Basic Dental and Medical Sciences, College of Dentistry, Ha'il University, Ha'il, Saudi Arabia, [2]Physical Biochemistry Research Laboratory, Biochemistry Department, Faculty of Science, University of Tabuk, Tabuk, Saudi Arabia, [3]Department of General Studies, Jubail Industrial College, Jubail Industrial City, Saudi Arabia, [4]Medical Research Centre, College of Applied Medical Sciences, Jazan University, Jazan, Saudi Arabia, [5]Department of Chemical Engineering, College of Engineering, Taibah University, Yanbu, Saudi Arabia

Introduction: Hydrogen peroxide plays a crucial role in melanogenesis by regulating tyrosinase activity, the key melanin-forming enzyme responsible for the browning of fruits, vegetables, and seafood. The need for effective solutions to mitigate such browning processes highlights the significance of developing advanced catalytic agents.

Methods: We synthesized highly effective FeSe$_2$ nanospheres using a one-step solvothermal process. The nanospheres were characterized through transmission electron microscopy (TEM), energy-dispersive X-ray analysis (EDX), and powder X-ray diffraction (XRD). Enzymatic activity was evaluated by plotting Michaelis-Menten and Lineweaver-Burk graphs to calculate the V$_{max}$ and K$_m$ parameters. Comparative analyses with a control sample and other known enzymes were performed to assess the catalytic efficiency.

Results and discussion: FeSe$_2$ nanospheres successfully catalyzed the reduction of hydrogen peroxide to water and alcohol, demonstrating enzyme-like activity. The initial reaction rate was 11 times higher than the control sample and significantly outperformed other enzymes, except for those relying on expensive noble metals. These nanospheres (termed Nanozymes) mimic the enzymatic action of natural antioxidants, such as the glutathione peroxidase (GPx) enzyme, in biological systems. Their exceptional efficiency makes them a strong candidate for practical applications in mitigating early browning caused by melanogenesis.

Conclusions: FeSe$_2$ nanozymes exhibit great promise as a biocatalyst for enhancing the shelf life of fruits and vegetables by reducing damage due to early melanogenesis. This cost-effective and efficient alternative to natural or noble metal-based enzymes offers significant potential for applications in food preservation and other industries.

GRAPHICAL ABSTRACT
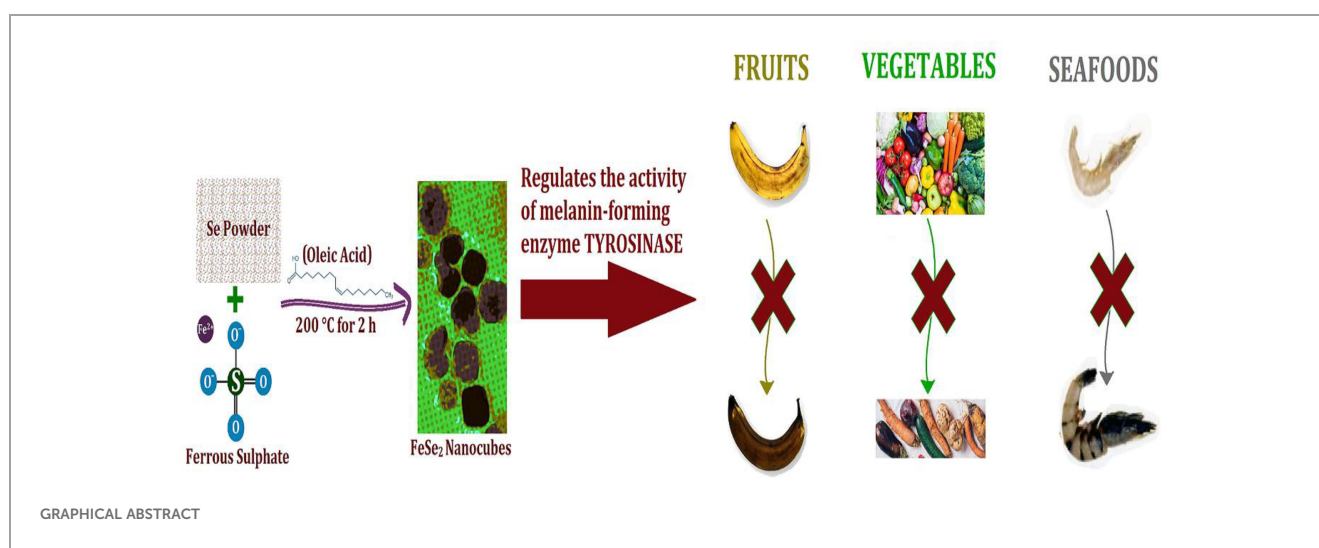
Introduction

Melanin is responsible for the hair, eye, and skin pigmentation (Costin and Hearing, 2007). Melanocytes produce melanin through a process known as melanogenesis (D'Mello et al., 2016; Videira et al., 2013). Tyrosinase, a well-known enzyme, and other tyrosinase-related proteins catalyze this process (Niu and Aisa, 2017). The abnormal loss of melanin causes vitiligo, a dermatological problem (Bergqvist and Ezzedine, 2020). Therefore, maintaining a balance between melanogenesis and tyrosinase activity is crucial for treating hypopigmentary disorders (Ferraro et al., 2021). Tyrosinase synthesizes melanin and finds extensive applications in the food industry (Parvez et al., 2007). This enzyme generates hydroxyl tyrosol, a food additive (Nawaz et al., 2017). The food manufacturing industries can utilize this to create the flavonoids in black tea, which have demonstrated anticancer qualities (Devi et al., 2020). Recently, researchers employed the tyrosinase enzyme to examine the proteins from chicken and pork (Lantto et al., 2007). There has been clear evidence of hydrogen peroxides and free radicals forming during the melanin process (Pilas et al., 1988). Observations reveal that the oxidation of certain phenolic precursors, like dopa-melanin and

dopamine-melanin, with oxygen from the air or hydrogen peroxide in basic media can produce melanins (d'Ischia et al., 2013; Jacobson, 2000). Thus, hydrogen peroxide regulation is critical for synthesizing melanins. A mismatch in the body's hydrogen peroxide concentration can lead to a decrease or increase in melanin production. There are multiple antioxidants and enzymes in the body that control the level of hydrogen peroxide, including glutathione (GSH) peroxidase (GPx) and cytochrome (Imai and Nakagawa, 2003). Researchers are working to develop to various artificial nano-materials (knowns as nanozymes) to mimic natural enzymes and also, they can control hydrogen peroxide production by neutralizing excess hydrogen peroxides (Abdelhamid et al., 2020; Abdelhamid and Sharmouk, 2023). Researchers have been making and using CuO@C, a transition metal-based chalcogenide, as one of the most promising nanozymes for the past few decades (Abdelhamid and Mahmoud, 2023; Lu et al., 2007). Researchers are experimenting with nanoparticles for various applications due to their outstanding qualities, including a high surface-to-volume ratio, tailorability for specific uses, and low dose requirement for action (Svendsen et al., 1972). Iron selenides are an important chalcogenide because they are relatively biocompatible and have favorable toxicological properties. Various forms of iron

selenides, including $FeSe_2$, FeSe, and Fe_7Se_8, exist (Sun et al., 2020). The stoichiometric ratio of iron to selenium ions determines the properties, including magnetic, optical, electrical, and catalytical activities (Lan et al., 2018; Coldea and Watson, 2018; Mohan et al., 2023). Thus, we can select the desired phase of iron selenide based on the intended applications.

The solution-phase approach is the preferred method for creating metal chalcogenides. Nowadays, the solution phase method has replaced the solid phase methods due to its ability to tailor the size, shape, and orientation of the nanomaterials to the desired application (Feng et al., 2004; Tahir et al., 2017). In addition to these advantages, the solution-phase synthetic method offers high purity and crystallinity as compared to the solid-state synthetic method. The hydrothermal and solvothermal methods are the two main techniques that fall under the solution phase method category. Qian et al. used the hydrothermal reduction route to synthesize the microcrystals of $FeSe_2$ and $FeTe_2$ and studied the magnetic properties (Costa et al., 2009). Mai et al. synthesized flower-like nanoparticles using the hydrothermal method. One drawback of these methods is that most of them employ the meticulously controlled autoclave. This research paper talks about a simple solvothermal method for making $FeSe_2$ nanospheres. It requires only one pot and uses ferrous sulfate ($FeSO_4$) and selenium powder as starting materials. We used different methods, like Transmission Electron Microscopy (TEM), Energy Dispersive X-ray analysis (EDX), and Power X-ray diffraction (XRD), to get a full picture of the synthesized nanospheres. The study also found that $FeSe_2$ nanospheres work like GPx enzymes do in living things, stopping the production of hydrogen peroxide by changing it into water and alcohol. This catalytic activity is particularly relevant in the context of melanogenesis, where hydrogen peroxide regulates the activity of

tyrosinase, a key enzyme involved in the production of melanin. The article also demonstrates that $FeSe_2$ nanospheres behave like enzymes by imitating the way natural antioxidants, such as the GPx enzyme, work. Because of their high surface area, the nanospheres help to balance the dysregulation of redox homeostasis, indicating potential therapeutic applications in managing oxidative stress. Furthermore, the research suggests that these $FeSe_2$ nanospheres could serve as a versatile nanodrug delivery system or carrier in the future. This implies that beyond their role as a catalyst for peroxide regulation, they could also serve as a platform for delivering therapeutic agents. In short, the article is mostly about making $FeSe_2$ nanospheres, characterizing them, and using them as catalysts to control peroxide. It also talks about their potential as antioxidant nanozymes and multifunctional nanodrug delivery systems.

Materials and methods

Instrumentation and characterization.

The $FeSe_2$ nanospheres were thoroughly characterized using TEM, EDX, and XRD. We conducted the TEM analysis using the Tecnai G2 20 instrument (FEI, Germany). Prior to any characterizations, we ultrasonicated the nanoparticles for an hour. For TEM analysis, we cast one drop of sample onto the TEM grid. Before the analysis, we allowed the TEM grid to dry overnight. We performed the EDX on a Zeiss EVO 50 scanning electron microscope from Germany. For the EDX analysis, the sample was drop-cast on the carbon tape and allowed to dry for one hour before analysis. We collected the XRD data of nanoparticles on X'Pert PRO (Netherlands). For the XRD analysis, we cast 25 mg of the sample onto glass slides. We scanned the glass

TABLE 1 A comparison between the activity of $FeSe_2$ nanospheres with previously reported nanozymes.

Nanozyme	Substrate	(K_m/mM)	V_{max}/$\mu M \cdot min^{-1}$	Experiential conditions	Ref.
Au25 clusterzyme	H_2O_2	–	470	GSH = 2 mM, NADPH = 200 mM, GR = 1.7 U·mL^{-1}, nanozyme = 10 ng·ML^{-1}	Liu et. al., 2021
Au24Cd1 clusterzyme	H_2O_2	–	100	–	Liu et. al., 2021
Au24Cu1 clusterzyme	H_2O_2	–	340	–	Liu et. al., 2021
Co/PMCS	H_2O_2	0.26	17.44	25°C, pH = 7.4, GSH = 2 mM, NADPH = 0.4 mM, GR = 1.7 U, nanozyme = 2.5 MM	Lai et. al., 2023
	GSH	2.81	12.97	–	Lai et. al., 2023
Se NPs	H_2O_2	0.200	13.51	25°C, GSH = 1.5 mM, NADPH = 1.25 mM, GR = 1 U, nanozyme = 0.5 mg·mL^{-1}	Chen et. al., 2021
GO-Se nanocomposite	H_2O_2	0.04	30	25°C, GSH = 2 mM, NADPH = 0.4 mM, GR = 1.7 U, nanozyme = 0.01 mg·mL^{-1}	Huang et. al., 2017
	GSH	0.72	49.2	–	
$FeSe_2$ nanospheres	H_2O_2	0.948	65.91	25°C, GSH = 0.1 M, NADPH = 0.2 mM, GR = 5 U, nanozyme = 25 mg·mL^{-1}	Present study
	GSH	2.377	106.38	–	

slides for two hours at temperatures ranging from 20 to 80 degrees. We also matched the data using the JCPDS file.

Synthesis of FeSe$_2$

We used the FeSO$_4$ and selenium powder as a precursor to synthesize FeSe$_2$ nanospheres. We used oleic acid as a solvent for this reaction. We maintained the stoichiometric ratio of Fe: Se at 1:2. We dispersed the selenium powder in oleic acid and heated it to 100°C for 1 hour. In oleic acid, we dropped the FeSO$_4$ dispersion into the selenium dispersion. We increased the reaction temperature to 200°C. We heated and stirred the reaction mixture for 6 hours. The reaction formed the black precipitate. We stopped the reaction and allowed it to cool down to room temperature. We collected the black precipitate using centrifugation and allowed it to dry overnight at room temperature. The black precipitate was thoroughly characterized using TEM, EDX, and XRD techniques.

Procedure of antioxidant behavior of FeSe$_2$

We assessed the antioxidant activity of the FeSe$_2$ nanospheres. We measured the activity using a UV-Vis spectrophotometer at a wavelength of 340 nm (Costa et al., 2009). We took 25 mg/mL of the nanoparticles in the cuvette. A pH of 7.4 and room temperature were used to add the 0.1 M GSH, 200 μM NADPH, 5 units of glutathione reductase, and 300 μM hydrogen peroxidase one at a time. Table 1 presents a comparison between the activity of FeSe$_2$ nanospheres with previously reported nanozymes (Jia et al., 2019; Liu et al., 2021; Lai et al., 2023; Chen et al., 2021).

Results

XRD, TEM, EDX

The solvothermal method synthesized FeSe$_2$ nanospheres using FeSO$_4$ and selenium powder as starting materials. The graphical abstract depicts the scheme for synthesizing iron chalcogenide nanoparticles. The experimental report mentions the detailed procedure. After synthesizing nanoparticles, the first step was to determine the shape, purity, and phase of the as-prepared nanoparticles. The TEM, EDX, and XRD techniques characterized the as-prepared nanoparticles.

XRD analysis

X-ray crystallography is a highly developed technique for determining the crystallinity, atomic structure, and molecular structure of a specimen. If the specimen is crystalline, the beam diffracts in many specific directions; otherwise, it passes straight into it without diffracting. Figure 1A shows the X-ray diffraction pattern of the prepared nanoparticles. The FeSe$_2$ planes (110), (011), (101), (111), (120), (211), (220), (031), and (122) correspond to the peaks at 24.2°, 30.1°, 31.7°, 34.8°, 36.7°, 44.2°, 48.1°, 51.7°, and 63.9°. All the assigned peaks are well-matched with respective JCPDS files 21-0432 (Huang et al., 2017; Zou et al., 2016). Figure 1B presents the theoretical XRD analysis. The experimental and theoretical XRD data both match well with each other. The XRD test also confirmed that the products were in the pure phase, which means that there were no other impurities in the diffraction peaks, like FeSe and selenium. The sharp peak in the XRD images also concludes that the synthesized nanoparticles have high
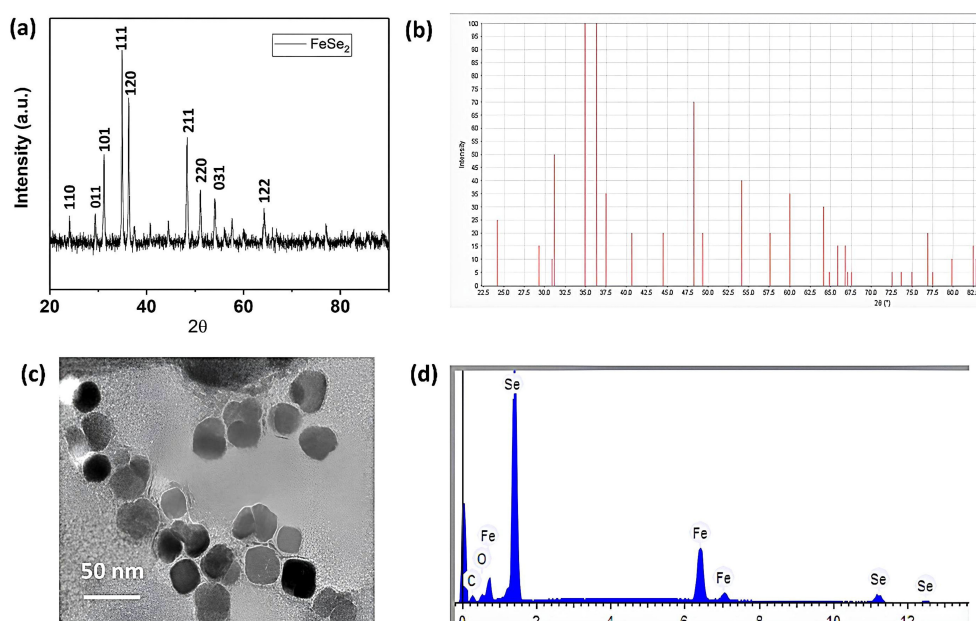
FIGURE 1
XRD, TEM & EDX analysis. **(A)** Experimental XRD data of FeSe$_2$ nanospheres; **(B)** theoretical XRD data of FeSe$_2$ nanospheres; **(C)** TEM scans of FeSe$_2$ nanospheres; **(D)** EDX images of FeSe$_2$ nanospheres.

crystallinity. The average crystalline size of the FeSe₂ nanospheres is 30 nm, according to our findings.

TEM analysis

We used transmission electron microscopy to determine the size and morphology of the synthesized nanoparticles. TEM is one of the most powerful techniques that uses an electron beam. The electron beam transmits through the sample to form a clear, bright, high-resolution image. This technique typically uses a specimen that is ultrathin, with a section size of less than 100 nm, or a suspension on the grid. As shown in Figure 1C, the shape of the nanoparticles appears to be cubic. We measured the size of the nanoparticles during the image-taking process. The average diameter of multiple images was taken, and it was ca. 18 ± 4 nm The nanoparticles (also referred to as nanospheres here) are uniformly distributed throughout. Furthermore, we observed no agglomeration during the sample scan.

EDX analysis

We used the EDX technique to determine the chemical composition and structure of nanospheres. This characterization technique involves depositing the specimen on a suitable substrate for analysis. We should choose a suitable substrate that does not interfere with the specimen's characterization. We chose the carbon tape as the substrate in this case and drop-casted the sample onto it. We kept the sample concentration low, approximately 10 mg/mL, to ensure a smooth composition determination. We scanned the

specimen in multiple areas and took into account the average results from all the pictures. As shown in Figure 1D, the EDX pattern confirmed the presence of iron, selenium, carbon, and oxygen elements. The carbon appears from the carbon tape (substrate), and oxygen is from atmospheric oxygen. As a result, the remaining peaks of iron and selenium confirmed the successful formation of FeSe₂ nanospheres. We used the instrumental automatic setup to determine the chemical composition and atomic percentage.

Table 2 displays the weights and atomic percentages detected by the EDX analysis. We found the weight percentages of iron and selenium to be 34.235 and 65.765, respectively. We found the atomic percentages of iron and selenium to be 33.452 and 66.548, respectively. Based on this observation, we calculate that the atomic percent ratio of Fe and Se is approximately 1:2, confirming the formation of FeSe₂ nanospheres. The EDX analysis detects no other impurities. The EDX data aligns well with the XRD data, confirming the sample's purity. XRD, TEM, and EDX results show that FeSe₂ nanospheres are element-free.

Discussion

Confirmation of FeSe₂

The XRD and EDX results show that FeSe₂ nanospheres form in the pure phase. These nanospheres have an average crystalline size of 30 nm. The average size of the nanospheres from TEM is found to be 18 to 22 nm, which is almost near the average size calculated from the PXRD. The nanoparticles exhibit a cubic shape and show no signs of agglomeration. Therefore, every test, including XRD, TEM, and EDX analyses, confirms the formation of FeSe₂ nanospheres. We assessed the antioxidant activity of FeSe₂ nanospheres for their potential antioxidant behavior. We studied the antioxidant activity using UV-Vis spectrophotometry (Ighodaro and Akinloye, 2018). The experimental section mentions the detailed procedure. We took 25 mg/mL of nanospheres in the cuvette, added all the ingredients stepwise, and monitored the absorption spectra at 340 nm. Figures 2A, B shows how the antioxidant activity of FeSe₂ nanospheres changes with UV light.

TABLE 2 Weight (%) and atomic (%) detections from EDX analysis of the FeSe₂ nanospheres.

EDX analysis		
Element	Weight (%)	Atomic (%)
Iron (Fe)	34.23	33.45
Selenium (Se)	65.76	66.54
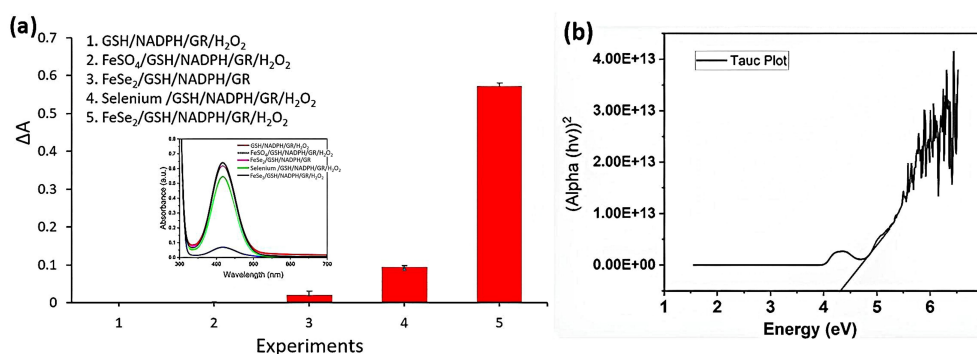
FIGURE 2
Activity profile. **(A)** Bar diagram showing difference in maximum absorbance along with all the experimental controls in GPx activities (Inset Figure UV-vis spectra of the GPx/antioxidant activity of FeSe₂ nanospheres). **(B)** Tauc plot of FeSe₂ nanospheres.

Over time, we see that adding nanospheres with GSH, NADPH, GR, and H2O2 makes the absorption peak at 340 nm go down by a large amount. However, in the absence of nanospheres, the absorption peak reduction rate at 340 nm is significantly lower and almost follows a straight line. The GPx is an antioxidant defense system that catalyzes and converts harmful hydrogen peroxide molecules into water or alcohol, thus protecting biomolecules from reactive oxygen species (Orian et al., 2015). Selenocysteine, which is present on GPx's active site, acts as a catalyst throughout the process without being consumed in the reaction (Walmsley et al., 1998).

We mixed the $FeSe_2$ nanospheres with all the other ingredients, except for GPx. We discovered that $FeSe_2$ can assist in converting hydrogen peroxide into water without depleting itself. The initial

rate of this antioxidant activity was found to be ca. 15.1 $\mu m\ min^{-1}$. We also determined the reaction rate in the absence of $FeSe_2$ nanospheres (control experiment). The reaction rate without $FeSe_2$ nanospheres comes out to be ca. 1.20 $\mu m\ min^{-1}$. This rate is approximately 11 times lower than that observed with the $FeSe_2$ nanospheres. It is also known that Fe can convert hydrogen peroxides into reactive oxygen species. We used all ingredients except glutathione reductase. Without the enzyme, the reaction rate dropped significantly to approximately 1.20 micrometers per minute. These results make it very clear that the catalytic activity happens when all of the necessary elements are present, such as $FeSe_2$, GSH, NAPHD, GR, and H2O2. In the absence of any of these components, the antioxidant activity does not occur, and the rate decreases significantly. This observation makes it clear that $FeSe_2$ nanospheres, like selenocysteine in living things, can speed up the reaction of hydrogen peroxide to water when all the other ingredients are present.

Steady-state kinetics analysis

Researchers also studied steady-state kinetics to understand substrate binding and structure-activity relationships (Jia et al., 2019). As shown in Figure 3, the catalytic reaction rate increases with the concentration of $FeSe_2$ nanospheres. This curve follows a straight line. In this regard, we ran two sets of experiments. In the First set, we vary the concentration of GSH (0–5 μM) by keeping the concentration constant of another substrate constant (Figure 4A), whereas in the next set we vary the concentration of H_2O_2 (0–1000 μM) by keeping the concentration There were no changes in the amounts of nanospheres, NADPH (200 μM), and GR (5 units) in the both set (Figure 4B). We have also plotted the Lineweaver-Burk plots with respect to GSH and H_2O_2 (Figures 5A, B).
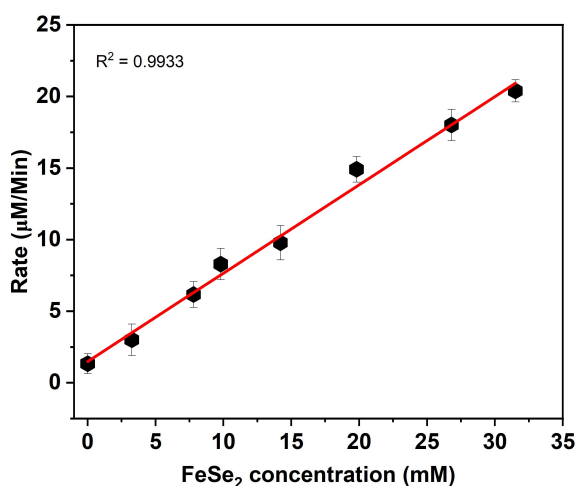
FIGURE 3
Liner relationship between $FeSe_2$ and rate in GPx activities. The rate was calculated by changing the concentration $FeSe_2$ (0-35 mM) by keeping the concentration constant of other co-factor/substrate.
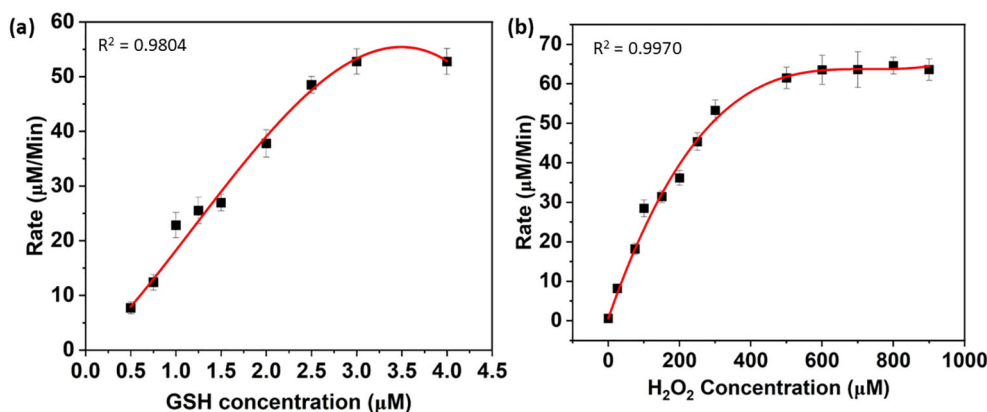
FIGURE 4
Michaelis-Menten kinetics corresponding to the variation of (A) GSH and (B) H_2O_2. In another set, the concentration of H_2O_2 was varied from 0 to 1000 μM, whereas the concentration of the other component was the same as mentioned before (B).
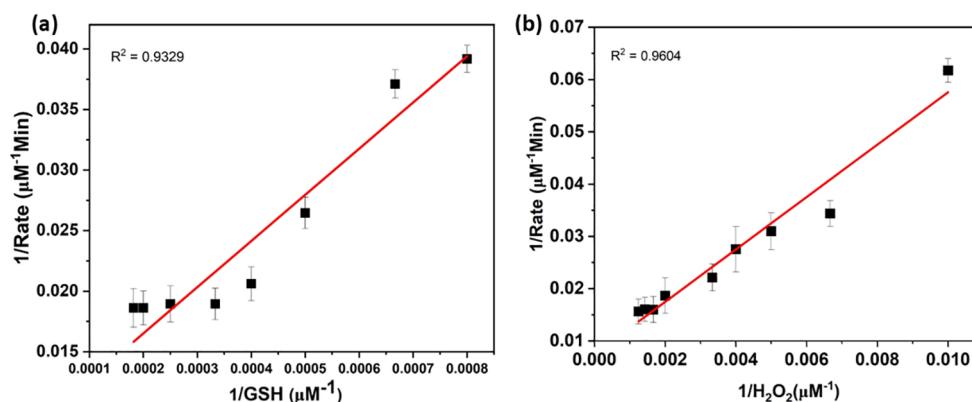
FIGURE 5
Michaelis-Menten kinetics of FeSe$_2$. Lineweaver-Burk plots of GPx activity of FeSe$_2$ corresponding to the variation of **(A)** GSH and **(B)** H$_2$O$_2$ concentration (plotted in Figure 4). Lineweaver-Burk plots were used to calculated the Michaelis constant K$_m$ values of GSH and H$_2$O$_2$. Here, 1/Rate represents the inverse of rate and 1/GSH and 1/H$_2$O$_2$ are the inverse of concentrations.

TABLE 3 K$_m$ and V$_{max}$ values of the FeSe$_2$ nanospheres.

Lineweaver-Burk plot analysis		
Antioxidants	K$_m$	V$_{max}$
Glutathione	2.3 mM	106.38 μM/min
H$_2$O$_2$	0.94 mM	65.91 μM/min

The K$_m$ and V$_{max}$

We calculated the K$_m$ and V$_{max}$ parameters from Lineweaver-Burk plots, and Table 3 mentions the values. The Vmax signifies the peak rate of the enzyme's kinetic reaction, which occurs when the substrate's active site reaches saturation (Naidja and Huang, 2002; Antony and Mohanan, 2019). Once the substrate reaches saturation, adding more substrate will not further increase the reaction rate. The K$_m$ represents the ease with which a substrate can saturate the enzyme. We found the K$_m$ and V$_{max}$ values for glutathione and hydrogen peroxide to be 2377.13 M and 948.06 M, respectively. Table 1 already compares the activity of the FeSe$_2$ nanospheres to previously reported nanozymes in the literature. We can say that FeSe$_2$ nanospheres are very good at fighting free radicals because they can quickly change H$_2$O$_2$ into H$_2$O, which is similar to how selenocysteine works at the GPx enzyme.

Conclusion

We produced the FeSe$_2$ nanospheres using the simple one-step solvothermal method. The nanospheres were thoroughly characterized using TEM, XRD, and EDX techniques. The TEM micrographs displayed the cubic shapes. The XRD analysis confirmed the Fe: Se composition to be 1:2, i.e., FeSe$_2$. Nanospheres were used as nanozymes to control hydrogen peroxide production, mimicking the action of the GPx enzyme in the human body. Nanospheres successfully convert hydrogen peroxide into water, similar to what selenocysteine does in the human body when GPx is present. We also determined the Vmax and Km parameters and generated both Michaelis-Menten and Lineweaver-Burk plots. These results clearly demonstrated the potential of FeSe$_2$ nanospheres for antioxidant applications, as well as their ability to reduce toxic hydrogen peroxide in water. Tyrosine can use these nanospheres as enzymes to control the production of hydrogen peroxide during the melanin synthesis process. This study may open up new doors for the food industry, as it is well known that tyrosine is responsible for the browning of fruits, vegetables, and seafood. Furthermore, the scientific community will greatly benefit if we can tailor these iron-based nanospheres, which are relatively biocompatible and exhibit favorable toxicological properties, to function as an efficient multifunctional nano-drug delivery system or carrier.

Data availability statement

The raw data supporting the conclusions of this article will be made available by the authors, without undue reservation.

Author contributions

SK: Conceptualization, Data curation, Formal analysis, Investigation, Methodology, Project administration, Writing – original draft, Writing – review & editing. SB: Funding acquisition, Investigation, Methodology, Software, Writing – original draft, Writing – review & editing. MA: Formal analysis, Investigation, Methodology, Resources, Writing – original draft, Writing – review & editing. IA: Data curation, Formal analysis, Investigation, Methodology, Writing – original draft, Writing – review & editing. MLo: Data curation, Formal analysis, Investigation, Methodology, Resources, Validation, Writing – original draft, Writing – review & editing. SR: Data curation, Methodology, Resources, Validation, Writing – original draft, Writing – review & editing. MLu: Formal analysis, Investigation, Methodology, Project administration, Supervision, Validation, Writing – original draft, Writing – review & editing.

Funding

Conflict of interest

The authors declare that the research was conducted in the absence of any commercial or financial relationships that could be construed as a potential conflict of interest.

Generative AI statement

The author(s) declare that no Generative AI was used in the creation of this manuscript.

Publisher's note

All claims expressed in this article are solely those of the authors and do not necessarily represent those of their affiliated organizations, or those of the publisher, the editors and the reviewers. Any product that may be evaluated in this article, or claim that may be made by its manufacturer, is not guaranteed or endorsed by the publisher.

References

Abdelhamid, H. N., and Mahmoud, G. A. E. (2023). Antifungal and nanozyme activities of metal-organic framework-derived cuO@C. *Appl. Organometallic Chem.* 37, e7011. doi: 10.1002/aoc.v37.3

Abdelhamid, H. N., Mahmoud, G. A. E., and Sharmouk, W. (2020). A cerium-based MOFzyme with multi-enzyme-like activity for the disruption and inhibition of fungal recolonization. *J. Materials Chem. B* 8, 7548–7556. doi: 10.1039/D0TB00894J

Abdelhamid, H. N., and Sharmouk, W. (2023). Intrinsic catalase-mimicking MOFzyme for sensitive detection of hydrogen peroxide and ferric ions. *Microchemical J.* 163, 105873. doi: 10.1016/j.microc.2020.105873

Antony, J., and Mohanan, P. V. (2019). Template synthesized polypyrroles as a carrier for diastase alpha amylase immobilization. *Biocatalysis Agric. Biotechnol.* 19, 101164. doi: 10.1016/j.bcab.2019.101164

Bergqvist, C., and Ezzedine, K. (2020). Vitiligo: a review. *Dermatology* 236, 571–592. doi: 10.1159/000506103

Chen, X., Zhu, X., and Gong, Y. (2021). Porous selenium nanozymes targeted scavenging ROS synchronize therapy, local inflammation, and sepsis injury. *Appl. Materials Today* 22, 100929. doi: 10.1016/j.apmt.2020.100929

Coldea, I., and Watson, M. D. (2018). The key ingredients of the electronic structure of FeSe. *Annu. Rev. Condensed Matter Phys.* 9, 125–146. doi: 10.1146/annurev-conmatphys-033117-054137

Costa, S., Schwaiger, S., and Cervellati, R. (2009). *In vitro* evaluation of the chemoprotective action mechanisms of leontopodic acid against aflatoxin B1 and deoxynivalenol-induced cell damage. *J. Appl. Toxicol.* 29, 7–14. doi: 10.1002/jat.v29:1

Costin, G. E., and Hearing, V. E. (2007). Human skin pigmentation: melanocytes modulate skin color in response to stress. *Fed. Am. Societies Exp. Biol.* 21, 976–994. doi: 10.1096/fj.06-6649rev

d'Ischia, M., Wakamatsu, K., and Napolitano, A. (2013). Melanins and melanogenesis: methods, standards, protocols. *Pigment Cell Melanoma Res.* 26, 616–633. doi: 10.1111/pcmr.2013.26.issue-5

D'Mello, A., Finlay, G. J., and Baguley, B. C. (2016). Signaling pathways in melanogenesis. *Int. J. Mol. Sci.* 17, 1144. doi: 10.3390/ijms17071144

Devi, P., Kaur, T., and Guleria, G. (2020). "Fungal secondary metabolites and their biotechnological applications for human health," in *New and future developments in microbial biotechnology and bioengineering* (Elsevier), 147–161.

Feng, J., Shen, D. Z., and Zhang, J. Y. (2004). High oriented FeSe thin film on GaAs (100) substrate prepared by low-pressure metal-organic chemical vapor deposition. *J. Magnetism Magnetic Materials* 279, 435–439. doi: 10.1016/j.jmmm.2004.02.030

Ferraro, M. G., Piccolo, M., and Pezzella, A. (2021). Promelanogenic effects by an Annurca apple-based natural formulation in human primary melanocytes. *Clinical Cosmetic Investigational Dermatol.* 14, 291–301. doi: 10.2147/CCID.S299569

Huang, Y., Liu, C., and Pu, F. (2017). A GO–Se nanocomposite as an antioxidant nanozyme for cytoprotection. *Chem. Commun.* 53, 13082–13085. doi: 10.1039/C7CC00045F

Ighodaro, M. I., and Akinloye, O. A. (2018). First line defence antioxidants-superoxide dismutase (SOD), catalase (CAT), and glutathione peroxidase (GPX): Their fundamental role in the entire antioxidant defence grid. *Alexandria J. Med.* 54, 287–293. doi: 10.1016/j.ajme.2017.09.001

Imai, H., and Nakagawa, Y. (2003). Biological significance of phospholipid hydroperoxide glutathione peroxidase (PHGPx, GPx4) in mammalian cells. *Free Radical Biol. Med.* 34, 145–169. doi: 10.1016/S0891-5849(02)01197-8

Jacobson, S. (2000). Pathogenic roles for fungal melanins. *Clin. Microbiol. Rev.* 13, 708–717. doi: 10.1128/CMR.13.4.708

Jia, Q., Zhang, Q., and Li, Z. (2019). Lateral heterojunctions within ultrathin FeS–FeSe2 nanosheet semiconductors for photocatalytic hydrogen evolution. *J. Materials Chem. A* 7, 3828–3841. doi: 10.1039/C8TA11456K

Lai, Y., Wang, J., and Yue, N. (2023). Glutathione peroxidase-like nanozymes: mechanism, classification, and bio-application. *Biomaterials Sci.* 11 (7), 2292–2316. doi: 10.1039/D2BM01915A

Lan, Y., Zhou, J., and Xu, K. (2018). Synchronous synthesis of Kirkendall effect induced hollow FeSe 2/C nanospheres as anodes for high performance sodium ion batteries. *Chem. Commun.* 54, 5704–5707. doi: 10.1039/C8CC02669F

Lantto, R., Puolanne, E., and Kruus, K. (2007). Tyrosinase-aided protein cross-linking: effects on gel formation of chicken breast myofibrils and texture and water-holding of chicken breast meat homogenate gels. *J. Agric. Food Chem.* 55, 1248–1255. doi: 10.1021/jf0623485

Liu, Y., Li, L., and Sun, S. (2021). Catalytically potent and selective clusterzymes for modulation of neuroinflammation through single-atom substitutions. *Nat. Commun.* 12, 114. doi: 10.1038/s41467-020-20275-0

Lu, H., Salabas, E. E., and Schüth, F. (2007). Magnetic nanoparticles: synthesis, protection, functionalization, and application. *Angewandte Chemie Int. Edition* 46, 1222–1244. doi: 10.1002/anie.200602866

Mohan, J., Kumar, R., and Roy, I. (2023). Iron Selenide Nanorods for light-activated anticancer and catalytic applications. *New J. Chem.* 47, 2527–2535. doi: 10.1039/D2NJ05094C

Naidja, A., and Huang, P. M. (2002). Significance of the Henri–Michaelis–Menten theory in abiotic catalysis: catechol oxidation by δ-MnO2. *Surface Sci.* 506, L243–L249. doi: 10.1016/S0039-6028(02)01375-4

Nawaz, T., Shafi, M., and Khaliq, A. (2017). Tyrosinase: sources, structure, and applications. *Int. J. Biotechnol. Bioengineering* 3, 142–148. doi: 10.25141/2475-3432-2017-5.0135

Niu, C., and Aisa, H. A. (2017). Upregulation of melanogenesis and tyrosinase activity: potential agents for vitiligo. *Molecules* 22, 1303. doi: 10.3390/molecules22081303

Orian, L., Mauri, P., and Roveri, A. (2015). Selenocysteine oxidation in glutathione peroxidase catalysis: an MS-supported quantum mechanics study. *Free Radical Biol. Med.* 87, 1–14. doi: 10.1016/j.freeradbiomed.2015.06.011

Parvez, S., Kang, M., and Chung, H. S. (2007). Naturally occurring tyrosinase inhibitors: Mechanism and applications in skin health, cosmetics, and agriculture industries. *Phytotherapy Res.* 21, 805–816. doi: 10.1002/ptr.v21:9

Pilas, T., Sarna, T., and Kalyanaraman, B. (1988). The effect of melanin on iron-associated decomposition of hydrogen peroxide. *Free Radical Biol. Med.* 4, 285–293. doi: 10.1016/0891-5849(88)90049-4

Sun, Z., Wu, X., and Gu, Z. (2020). Rationally designed nitrogen-doped yolk-shell Fe7Se8/Carbon nanoboxes with enhanced sodium storage in half/full cells. *Carbon* 166, 175–182. doi: 10.1016/j.carbon.2020.05.049

Svendsen, S. R., Åkesson, G., and Krogh-Moe, J. (1972). Decomposition pressures and standard enthalpy of formation for the iron selenides FeSe, Fe7Se8, Fe3Se4, and FeSe2. *Acta Chemica Scandinavica* 26, 3757–3774. doi: 10.3891/acta.chem.scand.26-3757

Tahir, B., Iqbal, T., and Hassan, A. (2017). Wet chemical co-precipitation synthesis of nickel ferrite nanoparticles and their characterization. *J. Inorganic Organometallic Polymers Materials* 27, 1430–1438. doi: 10.1007/s10904-017-0598-5

Videira, F. D. S., Moura, D. F. L., and Magina, S. (2013). Mechanisms regulating melanogenesis. *Anais Brasileiros Dermatologia* 88, 76–83. doi: 10.1590/S0365-05962013000100009

Walmsley, R., Barrett, M. P., and Bringaud, F. (1998). Sugar transporters from bacteria, parasites, and mammals: structure–activity relationships. *Trends Biochem. Sci.* 23, 476–478. doi: 10.1016/S0968-0004(98)01326-7

Zou, H., Sun, H., and Wang, L. (2016). Construction of a smart temperature-responsive GPx mimic based on the self-assembly of supra-amphiphiles. *Soft Matter* 12, 1192–1199. doi: 10.1039/C5SM02074C